Specific Impulse of Electric Solid Propellant in an Electrothermal Ablation-fed Pulsed Plasma Thruster

IEPC-2019-421

Presented at the 36th International Electric Propulsion Conference
University of Vienna • Vienna, Austria
September 15-20, 2019

Matthew S. Glascock,[1]
Missouri University of Science and Technology, Rolla, Missouri, 65409, USA

Joshua L. Rovey,[2]
University of Illinois Urbana-Champaign, Urbana, Illinois, 61801, USA

and

Kurt A. Polzin[3]
NASA Marshall Space Flight Center, Huntsville, Alabama, 35812, USA

Electric solid propellants are advanced solid chemical rocket propellants that can be controlled (ignited, throttled, and extinguished) through the application and removal of an electric current. Recent work has focused on application of this propellant in an electrothermal ablation-fed pulsed plasma thruster. In this paper, impulse bit measurements in such devices fed by either the electric solid propellant or a traditional state-of-the-art propellant, polytetrafluoroethylene, are expanded upon. It is demonstrated that a surface layer in the hygroscopic electric solid propellant is rapidly ablated over the first few discharges of the device, which correspondingly decreases specific impulse relative to the traditional polytetrafluoroethylene propellant. Correcting these data by subtracting the early discharge ablation mass loss measurements yields a corrected electric solid propellant specific impulse of approximately 300 s. As the test duration increases to a large number of discharges, and the initial mass loss is a reduced fraction of the total, the effect of absorbed water in the propellant is decreased and the specific impulse without any corrections approaches the corrected 300 s value.

I. Introduction

ELECTRIC solid propellants (ESPs) ignite and decompose when electric power is applied at sufficient current and voltage[1]. This decomposition is a highly exothermic process that generates hot gas at a burn rate that can be throttled by varying the applied current. Removal of the voltage and current extinguishes the reaction, which may be restarted by reapplication of electric power[2]. Because this reaction is only induced by electric current, ESPs are not susceptible to accidental ignition by spark, impact, or open flame. These characteristics are extremely beneficial

[1] NASA Space Technology Research Fellow, Aerospace Plasma Lab, msgdm3@mst.edu.
[2] Associate Professor of Aerospace Engineering, rovey@illinois.edu.
[3] Space Systems Team Lead, Advanced Concepts Office, kurt.a.polzin@nasa.gov.

compared to traditional solid rocket propellants, which are not throttleable, toggleable, or insensitive to external ignition. The advent of ESPs expands the potential applications for solid propellants that were previously infeasible.

Development of ESPs began in the 1990's with the design of an automobile air bag inflator propellant (ABIP) using materials safe for unprotected human contact (i.e., "green" materials). This ABIP was ammonium nitrate-based and was later repurposed for use in other areas, including rocket propulsion. Shortly thereafter, "ASPEN," the first digitally controlled extinguishable solid propellant, was developed[3]. This propellant featured additives with the ammonium nitrate base to lower melting point and increase electrical conductivity[2]. The material exhibited performance metrics comparable to that of previous solid rocket propellants, but major problems existed with the repeatability of ignition. Further development for gas-generation applications led to a special family of electrically controlled energetic materials which may be mixed to yield solid, liquid, or gel form propellants, all of which are electrically ignitable[4,5]. Some mixtures are flame-sensitive and explosive, some insensitive to flame and sustainable, and some are insensitive and extinguishable like the ESPs. One particular formula with high specific impulse and electrical conductivity is known as the high performance electric propellant, or HIPEP[1,6], which is not sensitive to open flame, spark, or impact, and is extinguishable. In this solid energetic material, the ionic liquid oxidizer hydroxyl-ammonium nitrate (HAN) is dissolved and cross-linked in polyvinyl alcohol (PVA), forming a gel that is hardened by baking. The resulting rubbery solid HIPEP exhibits a pyroelectric behavior unique to energetics. When direct current electric power is applied, a proton transfer reaction between hydroxyl-ammonium and nitrate is promoted, and the level of nitric acid rapidly rises in the material eventually triggering ignition of the propellant. This exothermic, gas-generating reaction may be harnessed in a solid rocket motor to generate on demand thrust using electric power.

HIPEP's pyroelectric behavior may facilitate a dual mode propulsion system using the solid propellant. The first mode is a high thrust chemical mode where direct current electric power is applied to incite pyroelectric gas generation. This gas is expanded through a nozzle to generate thrust like any typical solid rocket motor. The duration of each chemical mode activation is determined by the duration that electric power is supplied. The inventors of this propellant and collaborating groups have reported on this mode of operation[7-9]. Using a second circuit connected to the motor in parallel with the pyroelectric circuit, this solid rocket may also be operated in a high specific impulse (I_{sp}) electric mode. One promising electric mode circuit configuration is based upon a pulsed electric propulsion device known as the coaxial ablation-fed pulsed plasma thruster (APPT).

Pulsed plasma thrusters[10] (PPTs) have been in use since the first orbital flight of an electric propulsion device in 1964. PPTs offer repeatable impulse bits with higher exhaust velocities than can be achieved using chemical thrusters. Ablating polytetrafluoroethylene (PTFE) in the discharge to yield a working fluid, APPT's have the added benefit of inert propellant storage with no pressure vessel requirements. PPT's typically fulfill secondary propulsion needs such as station-keeping and attitude control on spacecraft, but have recently garnered more attention as a main propulsion for small spacecraft[11,12]. Broadly, PPT's may be classified as either rectangular or coaxial geometry[10]. Coaxial geometry APPT's, like that of the PPT-4[13], electrothermal PPT[14-18], or ablative z-pinch PPT[19], begin with a central and a downstream electrode and may have a conical-shaped discharge channel between the electrodes. The central or upstream electrode is typically cylindrical and positively charged (anode) while the downstream electrode is ring-shaped. Solid propellant fills the space between electrodes and may be fed from the side through the conical dielectric comprising the walls of the discharge channel. Most commonly this solid propellant is the inert polymer PTFE, which is the state-of-the-art propellant for APPTs. A capacitor or bank of capacitors is charged to a few kilovolts, with that voltage applied across the electrodes. The main arc discharge is initiated by an igniter, which is always located in or near the cathode in a PPT. The igniter generates a surface flashover discharge to create a seed plasma, initiating the main arc discharge. Radiation from this high temperature arc discharge heats the surface of the solid propellant, causing ablation of gaseous propellant species, further fueling the arc. The coaxial PPT is a device dominated by electrothermal acceleration mechanisms, with the energy of the arc heating the gas to yield high exit velocities through gas-dynamic acceleration. Ablation processes are at the core of APPT operation, and thus many studies on the ablation of PTFE exist in literature[20-25].

The aforementioned dual mode device combining a solid chemical rocket motor mode with an electric coaxial APPT mode remains conceptual. Research on the use of HIPEP and other ESPs for gas-generation and chemical mode applications with long (>1 ms) timescales is ongoing and separate from the present work. Current efforts by the authors are focused on understanding the behavior of the HIPEP material in the proposed APPT electric mode. Our recent work has compared the ablation of HIPEP with that of traditional PTFE tested in ablation-fed arc discharge devices[26-28]. At high temperatures and over long (~ms) time-scales, it is known that HIPEP undergoes a thermal decomposition process, while PTFE evaporates after depolymerization. However, ablation-controlled arc discharges occur on much shorter timescales, as the discharge current has a period of less than 10 μs. The specific ablation (μg/J)

of HIPEP was measured to be roughly twice that of PTFE, and this difference was attributed to differences in the thermal and chemical properties between the materials[26]. Plume measurements of HIPEP-fueled pulsed microthrusters[27] indicate electron temperatures (1-2 eV) and densities (10^{11}-10^{14} cm^{-3}) of the weakly ionized plasma that are comparable to PTFE-fueled APPTs. The measured exhaust velocities are comparable for microthrusters operating HIPEP or PTFE. Further, it has been shown that the fraction of late-time ablation mass is similar between propellants. Estimates from high-speed imagery of a pulsed HIPEP microthruster suggest that up to 50% of the mass ablated may be attributed to low-speed macroparticles ejected after the main current pulse[28].

Our most recent work investigated the performance of HIPEP in an electrothermal APPT device, where propellant material is ablated during a high current, short duration (~10 μs) arc discharge and accelerated by predominantly electrothermal mechanisms. The impulse bit (impulse-per-pulse) operating on PTFE and HIPEP was measured using an inverted pendulum thrust stand for both short and long-duration tests at stored energy levels ranging from 5-20 J. Results indicated that the impulse bit was nearly identical between propellants regardless of energy level, with HIPEP impulse bits typically 5% less than those for PTFE. Impulse bits at 5 J were ~100 μN-s and increased linearly by ~30 μN-s/J up to ~550 μN-s at 20 J. Measured mass loss for HIPEP was double that of PTFE, resulting in a calculated specific impulse of 225 s for HIPEP compared to 450 s for PTFE. However, it was postulated that because the first few pulses on HIPEP resulted in impulse bits that were typically 10-30% greater than the average over the first 100 pulses, that absorbed moisture or other surface impurities could be affecting mass loss (and thus specific impulse) measurements during those pulses. In the present work we investigate this behavior in greater detail. Very short duration tests are conducted to quantify the early-pulse mass loss, and the mass loss measurements in long-duration tests are closely examined for both PTFE and HIPEP propellant to identify long-term trends in the calculated specific impulse. We discuss the role of moisture absorbed by the hygroscopic HIPEP in mass loss measurements and specific impulse calculations, as well as its impact on future thruster designs.

II. Experimental Apparatus

A. High Performance Electric Propellant

HIPEP is a HAN-based solution solid manufactured by Digital Solid State Propulsion (DSSP) using "green" ingredients and processes free of harmful fumes. HIPEP has a chemical composition of 75% HAN oxidizer (an inorganic ionic liquid), 20% polyvinyl alcohol (PVA) fuel binder, and 5% ammonium nitrate. It is mixed in standard chemical glassware, with only gloves and safety glasses needed for protection, and cured at 35°C/95°F. It is initially a liquid and poured into a mold, curing to form a rubbery solid with density ~1.8 g/cm^3 and the appearance and texture of a soft pencil eraser. Our previous work has shown that HIPEP ablates more readily than PTFE in an ablation-fed arc, which we have shown that it is attributable to the differences in the thermodynamic properties of the solid propellant. Specifically, the decreased thermal degradation temperature and energy required to evolve propellant vapor lends to increased ablation of HIPEP relative to PTFE[26].

The solid HIPEP material is hygroscopic and gradually absorbs moisture from a typical laboratory atmosphere (~50% rel. hum.), eventually causing the propellant to become completely liquid. To mitigate absorption of moisture, HIPEP samples are handled and measured only in a dry-air glovebox kept at 5% relative humidity. The material is stored only in a vacuum or dry-air environment. Further, the test samples undergo a vacuum drying process wherein samples were kept at $<5\times10^{-2}$ torr for at least 24 h. After this time, samples have reached steady state and the measured mass is within 0.26% of the dry mass[26]. A Sartorius QUINTIX125D-1S dual range semi-micro balance was used to measure the mass of propellant samples before and after testing. In the selected range, this balance has a capacity of 60 g and can be read down to an increment of 0.01 mg. The factory reported repeatability of the balance is 0.02 mg. For measurements reported here the typical variation in measurement was ±0.03 mg.

B. Compact Thrust Stand

Testing was conducted in Electric Propulsion Facility 1 (affectionately named the "Burton chamber") at the University of Illinois Electric Propulsion Lab. This facility is approximately 1000 L in volume and achieves a base pressure of $\sim2\times10^{-5}$ torr. Housed in this facility is the UIUC compact thrust stand, which was designed for accurate measurement of thrust and impulse bit in the micro- and milli-Newton range[29]. The stand is of an inverted-pendulum design with a footprint of only 20x39 cm and 50 kg thruster mass capacity. Two modes of stand operation allow for constant thrust force measurement in the range of 1-10 mN and impulsive measurements in the range of 0.1-3.0 mN-s. In the present work the stand was operated in impulsive measurement mode to quantify the impulse-per-pulse, or

impulse bit, of a pulsed plasma device. Thrust stand calibration is performed using a method similar to the one described in Polk, *et al.*,[30] for impulsive measurements using an inverted-pendulum thrust stand. A remotely actuated impact hammer delivers an impulse of typically 100-1400 μN-s to the stand. The hammer directly strikes a piezo-electric force transducer, which measures the force imparted as a function of time. Integration of this signal yields the impulse imparted to the stand. Each strike of the hammer generates oscillatory motion of the thrust stand, which is measured by a linear variable differential transformer (LVDT). The integrated force signals and associated stand response measurements are then combined to establish a calibration curve of stand response as a function of known impulse which may be used to determine a single impulse bit within ±20 μN-s. Further details and a sample calibration curve may be found in a recent previous publication[31].

C. Electric Propellant Thruster Experiment

The electric propellant thruster experiment (EPTX) used in this work and shown schematically in Figure 1 has a geometry similar to that of a coaxial electrothermal APPT. It should be noted that this device was originally used primarily to study the mass ablation of the propellants and not as a thruster[26]. The device was designed to facilitate removal and replacement of small propellant tube samples and is not optimized for performance. More recently, the device was modified with by adding a 15° conical nozzle shape in the stainless steel cathode in an attempt facilitate gasdynamic expansion to better utilize the thermal energy imparted to the plasma by the arc discharge. A circular stainless steel rod located upstream serves as the anode (positive electrode) and the assembly is housed in a nonconductive PEEK body. The propellant tube sample has length 12 mm and inner diameter 6.35 mm. During operation, up to ~2.3 kV is applied between the anode and cathode, which is not high enough to produce a breakdown under vacuum conditions. The device is triggered by a surface discharge igniter embedded in the nozzle of the cathode. A capacitor discharge ignition (CDI) circuit creates a low energy surface discharge between the tungsten wire tips. Electrons from this discharge are accelerated to the positively charged anode and sputter particles from the electrode and the nearby propellant, promoting the main arc discharge in the cavity formed by the propellant tube inner wall and the anode end.

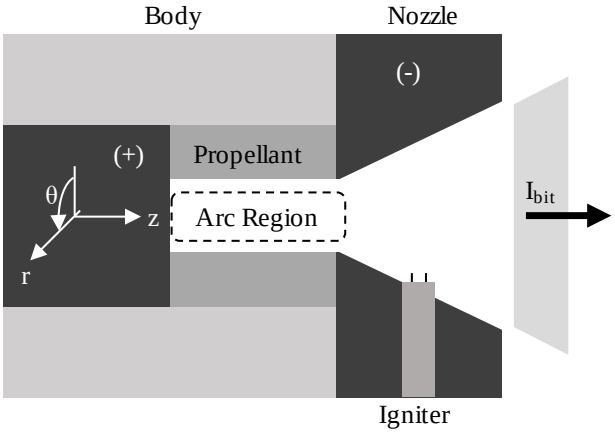

Figure 1: Diagram of the electric propellant thruster experiment.

During the main arc discharge high current flows between the anode and cathode, oscillating around zero with the same form of an underdamped inductance-capacitance-resistance series circuit possessing a period of a few microseconds. In this device, the Lorentz force is directed in the negative radial direction (pinching toward the *z*-axis) in the arc region. In the conical nozzle region, a radial component of current may give rise to a small electromagnetic thrust component, but the device is known to be primarily electrothermal. The energy that was initially stored in the capacitors is deposited in the plasma through resistive dissipation. This energy transiently heats the walls of the propellant cavity to well above the vaporization temperature and causes ablation of propellant at a rate of between ~30-300 μg/pulse, dependent upon the discharge energy. The gas generated by ablation is then further heated by the arc discharge to high temperatures on the order of a few eV. This mass of high temperature charged particles and neutrals is accelerated gas-dynamically via the nozzle to impart an impulse per pulse or impulse bit (I_{bit}). In the present work the device is triggered at a repetition rate of once per ~20 seconds. This low repetition rate means the propellant has time to cool before the next discharge is initiated.

III. Experimental Approach

We first summarize the significant findings from a previous experimental investigation to frame the approach used in the present work. In the previous work, short duration constant discharge energy test runs of 100 pulses were conducted in the EPTX device with both PTFE and HIPEP. The impulse bit was measured for testing at nominal discharge energy levels of 5, 10, 15 and 20 J. A representative impulse bit data set acquired during the course of one test on each propellant is shown in Figure 2a. These data have been normalized by the average impulse bit values for their respective 100 pulse sets. We observe for both propellants that after a short initial transient the impulse bit stabilizes, varying about the mean and remaining roughly constant, within the error bars (±20 μN-s), for pulses 10-100. During the initial transient, the impulse bit for the first pulse of each test run is 30-40% greater than the average and decreases in each subsequent trial for pulses 2-10 until a rough steady state is achieved near the average value. This phenomenon of initially high and then decreasing impulse bits as the propellant surface is conditioned over the first few pulses has previously been observed in the literature for PTFE[16,19].

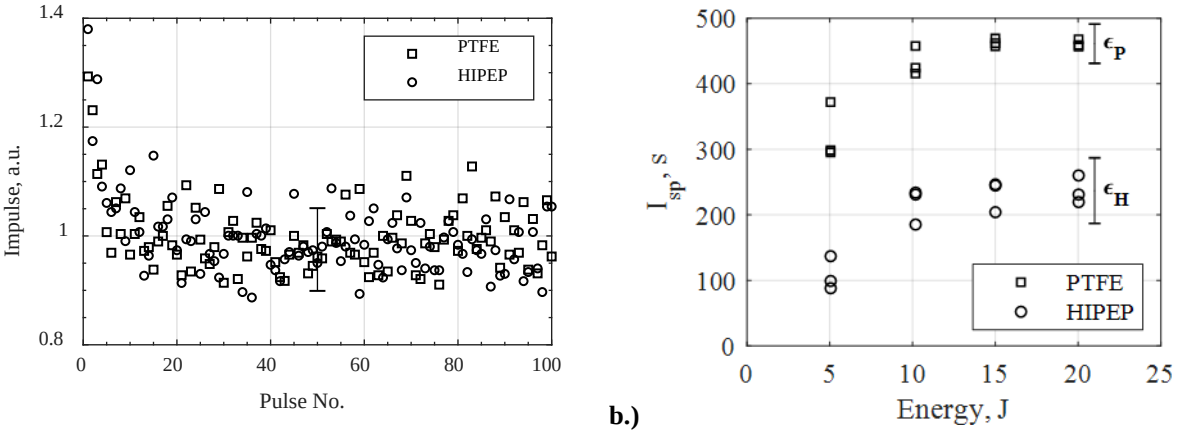

a.) **b.)**

Figure 2: Summary of results from Ref. [31]. a.) Impulse bit measurements over short duration tests representative of most trials and normalized by the average impulse bit values for each set, and b.) Average specific impulse as a function of discharge energy for each short-duration tests as a function of propellant type and discharge energy (representative error bars are shown for HIPEP (ϵ_H) and PTFE (ϵ_P)).

The mass of each propellant sample was measured directly before and after a test run to determine the net ablation mass loss during each test. Special preparation procedures[26] were followed to evaporate absorbed moisture in the hygroscopic HIPEP material. In general, ablation mass increased in a linear fashion as a function of discharge energy. For PTFE, the ablation mass at 5 J was 35.3 μg/pulse which yielded a specific ablation of ~7 μg/J. For the other, higher energy levels, the specific ablation was on average a constant ~6.3 μg/J. HIPEP ablation exhibits similar scaling, but at a specific ablation rate that is much greater than PTFE. At 5 J, the ablation mass of HIPEP is on average 106.8 μg/pulse or ~21 μg/J, which is about three times that of PTFE. The specific ablation of HIPEP decreases to about 12.5 μg/J at the higher discharge energy levels tested. This is roughly twice that of PTFE. Also reported in the previous work was the average specific impulse, or I_{sp}. This quantity is expressed in seconds and is defined as the total impulse for a test run divided by the total weight of propellant expelled during the test. This is written as

$$I_{sp} = \frac{I_{total}}{m g_0} \tag{1}$$

where I_{total} is the sum of all impulse bit measurements for a given test run, m is the ablation mass loss during a given test run, and g_0 is the acceleration due to gravity. Since the measured impulse bits at all energy levels are nearly identical between the two propellants, the higher mass ablated per pulse results in a specific impulse for HIPEP that is significantly lower than for PTFE. Shown in Figure 2b are the average I_{sp} values calculated using Eq. (1) for both propellants over several short-duration (100 pulse) test trials. The measurement error for HIPEP (ϵ_H) specific impulse is ±50 s and for PTFE, the measurement error (ϵ_P) is ±30 s. These errors are shown as representative error bars in the figure. On average from 10-20 J, the specific impulse for PTFE is calculated to be ~450 s compared to ~225 s for HIPEP.

Two key observations in the above results influenced the present work. First, the increased impulse bit over pulses 1-10 indicated some form of propellant surface conditioning was occurring. Our initial hypothesis was that the ablation mass loss was also greater during these pulses, but we could not definitively test this hypothesis because only average mass loss data over the full 100 pulse duration of each test was available. Consequently, in the present work we performed very short duration tests of only 10 pulses to better quantify the early-pulse mass losses. The aim is to understand the mass loss during the early pulses for and gain further insight into the increased ablation of HIPEP relative to PTFE.

Finally, it was noted in our original tests that the 5 J energy level specific impulse values for both propellants is significantly decreased relative to the higher energy levels. While the exact cause of the reduction at the low energy is currently unknown, it is suspected that the stored energy is insufficient to sustain a uniform arc discharge in the given cavity geometry. As a result, the arc would be either incomplete or non-uniform, causing non-uniform wall ablation and heating of propellant in the cavity. Therefore, many of the observations in the present paper may only be valid for the 10-20 J energy range, and may not hold for lower energy discharges.

IV. Results

The EPTX was tested using PTFE and HIPEP as propellants. In addition to the short-duration tests consisting of 100 pulses each and long-duration tests to end-of-life, both of which were reported in Ref. [31], in the present work we conducted very-short-duration tests consisting of 10 pulses. In this section, we present the results of these very-short-duration tests and compare those results to the 100 pulse short duration test results. First, a typical short-duration test at a single initial energy value, and then the average impulse bit over the short-duration tests at each energy level for both propellants are presented. Finally, the trend of impulse bit over the long-duration tests and the average impulse bit-per-joule of initial stored energy over the test duration is presented.

Testing and sample preparation procedures for very-short-duration 10 pulse tests were identical to those of the short-duration (100-pulse) tests and earlier ablation mass tests[26]. Samples are stored in rough vacuum for 24 h directly prior to mass measurement allowing absorbed water to evaporate. The initial sample mass is measured directly after vacuum drying and before loading into the EPTX device. After testing and another 24 hours of post-test vacuum drying, the final mass is measured. The ablation mass loss for the trial is the difference between initial and final masses. Results for 10-pulse trials at each energy level are shown in Table I alongside the average mass loss measured for 100-pulse trials. Also shown in the final column of Table I is the 10-pulse mass loss as a percent of the 100-pulse mass loss.

Table I: Ablation mass loss for 10- and 100-pulse tests.

Propellant	Energy, J	Total 10-pulse mass loss, mg	Total 100-pulse mass loss, mg	Ratio of 10-pulse to 100-pulse mass loss, %
PTFE	5.05	0.37	3.53	10.5%
	10.18	0.70	6.91	10.1%
	15.00	1.00	9.47	10.6%
	20.03	1.28	12.48	10.3%
HIPEP	5.05	5.82	10.68	50.7%
	10.18	6.42	13.33	48.2%
	15.00	6.02	18.43	32.7%
	20.03	6.14	26.06	23.6%

In Table I we observe at similar conditions that the mass loss for HIPEP is significantly greater than for PTFE. In 100-pulse tests, HIPEP mass loss is typically about twice that of PTFE. This is much greater in the 10-pulse tests, where the HIPEP mass loss is nearly six times that of PTFE. Second, while the mass loss of PTFE clearly increases with energy in 10-pulse trials, the same is not observed for HIPEP. Rather, the 10-pulse mass loss data for HIPEP appears to be independent of stored energy and is, on average, ~6 mg. Finally, we note that for all energy levels, the 10-pulse mass loss is 10-11% of the 100-pulse mass loss for PTFE. This result indicates that PTFE mass loss is roughly constant for both the 10-pulse and 100-pulse intervals. For HIPEP, the mass loss during 10-pulse tests is much greater than 10% in all cases, indicating that much of the mass lost during the 100-pulse tests was lost during the first 10 pulses.

V. Analysis and Discussion

The phenomenon of initially high and then decreasing impulse bits over the first few pulses has previously been observed in the literature for PTFE fueled ablation-fed devices[16,19]. The propellant surface is conditioned by the transient heating from the adjacent arc discharge resulting in the removal of impurities during those pulses. These impurities may be foreign particles on the surface acquired through handling or contact with a non-vacuum atmosphere. While PTFE is not porous or hygroscopic, it is expected that a small amount of moisture may reside on the surface as an impurity of the material before being subjected to the vacuum. These impurities add mass to the initial measurements, but evaporate or are expelled quickly during the first few pulses. In Table I we see that the first 10 pulses with PTFE exhibit a mass loss-per-pulse that is about 1% higher than the next 90 pulses. This indicates that the mass of impurities that are then expelled during propellant conditioning is quite small compared to the mass loss due to arc discharge ablation. Furthermore, a summation of the impulses in Figure 2a reveals that the sum total impulse for the first 10 pulses is about 10.8% of the sum total impulse for all 100 pulses. The additional mass (<1%) expelled due to surface impurities roughly translates to a relative increase of impulse (<1%) in the early pulses, indicating that on average the impurities are likely liberated by the arc discharge and accelerated to near the bulk plasma velocity.

As seen in Table I for HIPEP, the mass loss-per-pulse during pulses 1-10 is much greater than that of the 90 subsequent pulses. In the most extreme case, at 5 J, the mass lost in the first 10 pulses is more than 50% of the total mass loss over an entire 100 pulse test. However, using the data in Figure 2a, the sum total impulse for the first 10 pulses is only 10-11% of the sum total impulse from all 100 pulses. These combined observations indicate first that HIPEP not has more mass loss attributed to surface impurities (and thus more mass loss in earlier pulses) relative to PTFE. They also indicate that the average gas velocity of these first few pulses is significantly reduced because the impulse bit remains unchanged. Because HIPEP is extremely hygroscopic, we attribute this phenomenon to water absorbed into the propellant. The propellant preparation procedure appears to effectively remove a considerable amount of water (typically 5-6% propellant mass) by allowing it to slowly evaporate when exposed to vacuum conditions. It is possible that some water is able to absorb deeper into the fibers of the material, rather than just the surface. This deeply absorbed water would typically require a greater amount of time to evaporate in vacuum. The addition of thermal energy through arc discharge heating would greatly increases the evaporation rate and the commensurate mass loss rate. However, the fraction of early mass loss is significant and the vacuum drying process is sophisticated so we expect that a majority of the absorbed water is released during this preparation. Prior to drying, the absorbed water molecules may chemically react with the propellant resulting in a surface layer of unknown chemical composition and thickness. This layer of unknown chemical composition would not revert back to the original chemical composition of the propellant through a drying process. It is possible that this layer, which would be adjacent to the arc discharge for early pulses of a test, could ablate more readily than the standard propellant composition.

The mass loss measurement for HIPEP is skewed artificially high because of the very high mass loss rates in the early pulses. As a result, commensurate specific impulse calculations for the duration of the test are skewed lower. In the interest of reporting a specific impulse that is ideally achievable, we develop a simple method to correct the average mass lost data. Specifically, we subtract the mass loss and total impulse measured in first 10 pulses from results for 100-pulse mass loss and total impulse measurements, and then perform all the calculations to obtain the average mass loss-per-pulse and average corrected I_{sp} using those remaining 90 pulses from the 100-pulse test. The 100 pulse average I_{sp} values from Figure 2b and the and corrected values for HIPEP are shown in Figure 3.

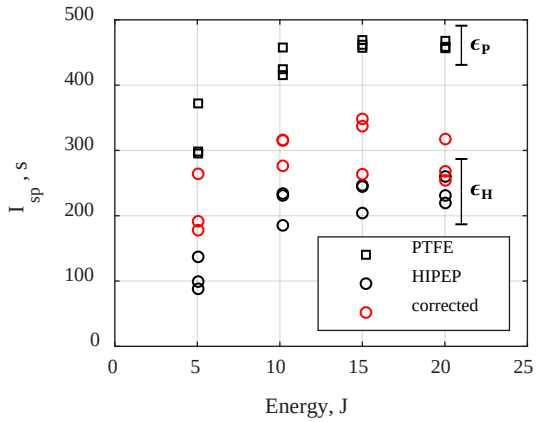

Figure 3: Average specific impulse as a function of discharge energy for each short-duration tests as a function of propellant type and discharge energy, with both raw and corrected HIPEP data.

In Figure 3 we observe that the corrected I_{sp} for HIPEP is greater than or equal to the previously measured values at each energy level. In fact, all but one corrected value at 20 J is greater than all of the previous results at that energy. This is the expected result, based upon the observation that a significant fraction sometimes constituting a majority of the mass is lost in early pulses. When we ignore this poor propellant utilization in early pulses, the overal specific impulse increases. At ≥10 J, the mean corrected I_{sp} is ~300 s, with the data scattered relatively uniformly about that value. As before, the mean corrected I_{sp} at the 5 J is reduced when compared to the higher energy data, with an average value of 211 s.

In the long-duration testing, the thruster was operated until the trigger pulse could no longer initiate a discharge[31]. As the number of discharges increase, the overall mass loss for an experimental data set will be larger and the initial mass loss for the first 10 pulses would become a decreasingly-small portion of the overall mass loss. Consequently, we expect that the average mass loss-per-pulse based on pre- and post-test mass measurements of the propellant will start to approach the corrected average mass loss-per-pulse obtained for pulses 11-100 of the 100-pulse tests. We can also use the same method (subtract from the data set the mass loss and total impulse measured in first 10 pulses) to correct the long-duration test data to quantify the effect of increased initial mass bits on calculated specific impulse. In Figure 4 we present for both HIPEP and PTFE the raw average specific impulse values for the 10, 15, and 20 J pulse energies as a function of number of pulses in the test for the very-short (10 pulse), short (100 pulses), and long-duration (1000+ pulses) tests. Representative error bars for short-duration PTFE (ϵ_P) and HIPEP (ϵ_H) specific impulse calculations are shown. We also present in Figure 4 for HIPEP tests the corrected specific impulse for short- and long-duration tests.

We observe that the raw calculated specific impulse of HIPEP does indeed appear to asymptotically approach the corrected value as pulse number increases. In the long-duration tests (1,000+ pulses), we find that the corrected specific impulse for HIPEP is very similar to the raw calculated value. As an illustration of this, the longest duration test on HIPEP involved 5,474 pulses at 20 J. This resulted in an overall mass loss of 788 mg and the total impulse 2.31 N-s, which yeilds a raw average specific impulse of roughly 300 s. The typical mass loss for the very-short 10-pulse duration test conducted at 20 J was 6 mg and total impulse was approximately 5 mN-s. These values are both less than 1% of the long-duration test totals, limiting their overall influence on the average specific impulse calculated using the long-duration test data. As a check, applying the correction by removing contribution of the first 10 pulses to the overall mass loss and total impulse has minimal effect, with the corrected specific impulse remaining roughly 300 s.

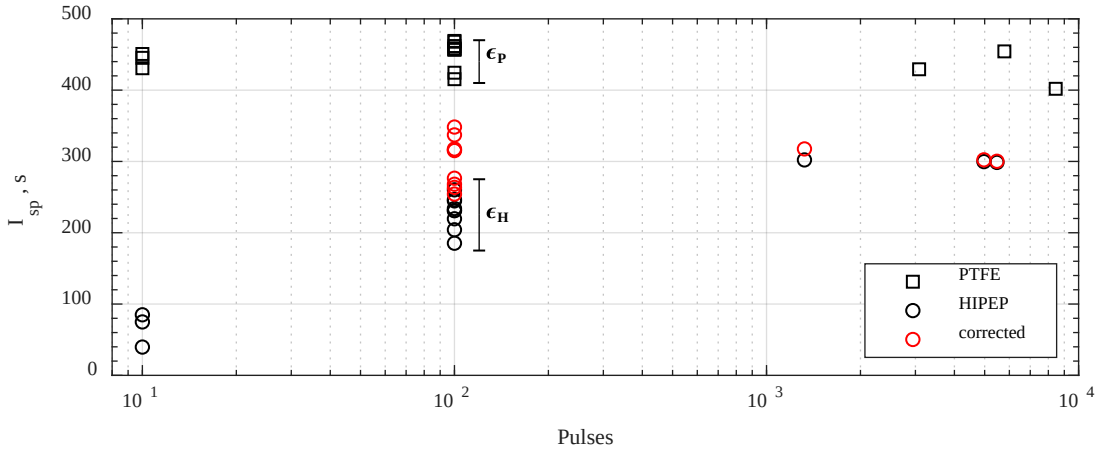

Figure 4: Average specific impulse as a function of test duration and propellant type, both raw values and corrected HIPEP data for the short- (100 pulses), and long-duration (1000+ pulses) tests.

VI. Conclusion

We have presented impulse and total mass loss measurements for an electric solid propellant known as HIPEP tested for different numbers of pulses and compared this testing with data obtained under similar conditions for operation on PTFE. The average specific impulse for PTFE was calculated from the total mass loss and impulse measurements, and it was found to be relatively constant for a given discharge and not dependent on total pulses. This implied relatively constant surface conditions for PTFE. The HIPEP propellant is significantly different in that it is a hygroscopic material and absorbed water greatly affects the experimental results. Drying the material by exposure to vacuum allows much of the absorbed water to evaporate over about 24 h. However, there are residual effects from the water that was absorbed by the propellant. In a coaxial ablation-fed PPT, the result is vastly increased ablation mass loss in the first several arc discharges near the surface. The mass loss in these early pulses is up to 50% higher than later in the device lifetime, but the total impulse during these pulses is only 10% increased. These observations are attributed either to the evaporation of deeply absorbed water remaining in the propellant or a reaction of the propellant surface with absorbed water to form a surface layer that decomposes and ablates in the presence of a high-current discharge more readily than the HIPEP material exposed after the surface layer is removed. As a result, the average specific impulse for 100-pulses tests on HIPEP was only 225 s. Correcting these data by removing the contributions of the first ten pulses from the data set yielded an average specific impulse of 300 s. Increasing the test duration to thousands of pulses significantly diminished the effect early, high-mass-loss pulses had on the average specific impulse. In the long-term tests the average specific impulse is roughly the same as the value obtained from the 100-pulse tests when those data are corrected for the contributions of the first 10 pulses.

Acknowledgments

M.S. Glascock would like to graciously thank the NASA Space Technology Research Fellowship program for funding his graduate research via grant NNX15AP31H. This work is a large part of that research and would not be possible without the support from this program. Additionally, the authors wish to thank DSSP for providing the HIPEP material in custom-made form for our research, as well as numerous discussions on the nuances of HIPEP operation and handling.

References

[1]Sawka, W. N., and McPherson, M., "Electrical Solid Propellants: A Safe, Micro to Macro Propulsion Technology," *49th Joint Propulsion Conference*, AIAA, San Jose, CA, 2013. doi: 10.2514/6.2013-4168

[2]Sawka, W. N., U.S. Patent for a "Controllable Digital Solid State Cluster Thrusters for Rocket Propulsion and Gas Generation," No. 7958823 B2 and 8464640; June 14, 2011 and June 18, 2013.

[3]Dulligan, M., U.S. Patent for a "Electrically Controlled Extinguishable Solid Propellant Motors," No. 7788900B2; September 7, 2010.

[4]Chung, K., Rozumov, E., Kaminsky, D., Buescher, T., Manship, T., Valdivia, A., Cook, P., and Anderson, P., "Development of Electrically Controlled Energetic Materials," *ECS Transactions*, Vol. 50, No. 40, 2013, pp. 59-66. doi: 10.1149/05040.0059ecst
[5]Grix, C., and Sawka, W. N., U.S. Patent for a "Family of Modifiable High Performance Electrically Controlled Propellants and Explosives," No. 8888935B2; November 18, 2011.
[6]Sawka, W. N., and Grix, C., U.S. Patent for a "Family of Metastable Intermolecular Composites Utilizing Energetic Liquid Oxidizers with Nanoparticle Fuels in Sol-Gel Polymer Network," No. 8317953B2; November 27.
[7]Baird, J. K., Lang, J. R., Hiatt, A. T., and Frederick, R. A., "Electrolytic Combustion in the Polyvinyl Alcohol Plus Hydroxylammonium Nitrate Solid Propellant," *Journal of Propulsion and Power*, Vol. 33, No. 6, 2017, pp. 1589-1590. doi: 10.2514/1.B36450
[8]Hiatt, A. T., and Frederick, R. A., "Laboratory Experimentation and Basic Research Investigation Electric Solid Propellant Electrolytic Characteristics," *52nd AIAA/SAE/ASEE Joint Propulsion Conference*, AIAA, Salt Lake City, UT, 2016. doi: 10.2514/6.2016-4935
[9]Sawka, W. N., and Grix, C., U.S. Patent for a "Electrode Ignition and Control of Electrically Ignitable Materials," No. 8857338B2; October 14.
[10]Burton, R. L., and Turchi, P. J., "Pulsed Plasma Thruster," *Journal of Propulsion and Power*, Vol. 14, No. 5, 1998, pp. 716-735. doi: 10.2514/2.5334
[11]Gatsonis, N. A., Lu, Y., Blandino, J., Demetriou, M. A., and Paschalidis, N., "Micropulsed Plasma Thrusters for Attitude Control of a Low-Earth-Orbiting Cubesat," *Journal of Spacecraft and Rockets*, Vol. 53, No. 1, 2016, pp. 57-73. doi: 10.2514/1.A33345
[12]Keidar, M., Zhuang, T., Shashurin, A., Teel, G., Chiu, D., Lukas, J., Haque, S., and Brieda, L., "Electric Propulsion for Small Satellites," *Plasma Physics and Controlled Fusion*, Vol. 57, No. 1, 2015, pp. 1-10. doi: 10.1088/0741-3335/57/1/014005
[13]Bushman, S., and Burton, R. L., "Heating and Plasma Properties in a Coaxial Gasdynamic Pulsed Plasma Thruster," *Journal of Propulsion and Power*, Vol. 17, No. 5, 2001, pp. 959-966. doi: 10.2514/2.5849
[14]Cheng, L., Wang, Y., Ding, W., Ge, C., Yan, J., Li, Y., Li, Z., and Sun, A., "Experimental Study on the Discharge Ignition in a Capillary Discharge Based Pulsed Plasma Thruster," *Physics of Plasma*, Vol. 25, No. 9, 2018. doi: 10.1063/1.5038087
[15]Wang, Y., Ding, W., Cheng, L., Yan, J., Li, Z., Wang, J., and Wang, Y., "An Investigation of Discharge Characteristics of an Electrothermal Pulsed Plasma Thruster," *IEEE Transactions on Plasma Science*, Vol. 45, No. 10, 2017, pp. 2715-2724. doi: 10.1109/TPS.2017.2738330
[16]Aoyagi, J., Mukai, M., Kamishima, Y., Sasaki, T., Shintani, K., Takegahara, H., Wakizono, T., and Sugiki, M., "Total Impulse Improvement of Coaxial Pulsed Plasma Thruster for Small Satellite," *Vacuum*, Vol. 83, No. 1, 2008, pp. 72-76. doi: 10.1016/j.vacuum.2008.03.082
[17]Edamitsu, T., and Tahara, H., "Experimental and Numerical Study of an Electrothermal Pulsed Plasma Thruster for Small Satellites," *Vacuum*, Vol. 80, No. 11, 2006, pp. 1223-1228. doi: 10.1016/j.vacuum.2006.01.055
[18]Miyasaka, T., Asato, K., Sakaguchi, N., and Ito, K., "Optical Measurements of Unsteady Phenomena on Coaxial Pulsed Plasma Thrusters," *Vacuum*, Vol. 88, 2013, pp. 52-57. doi: 10.1016/j.vacuum.2012.04.003
[19]Markusic, T. E., Polzin, K. A., Choueiri, E. Y., Keidar, M., Boyd, I. D., and Lepsetz, N., "Ablative Z-Pinch Pulsed Plasma Thruster," *Journal of Propulsion and Power*, Vol. 21, No. 3, 2005, pp. 392-400. doi: 10.2514/1.4362
[20]Keidar, M., Boyd, I. D., and Beilis, I. I., "Electrical Discharge in the Teflon Cavity of a Coaxial Pulsed Plasma Thruster," *IEEE Transactions on Plasma Science*, Vol. 28, No. 2, 2000, pp. 376-385. doi: 10.1109/27.848096
[21]Keidar, M., Boyd, I. D., and Beilis, I. I., "Model of an Electrothermal Pulsed Plasma Thruster," *Journal of Propulsion and Power*, Vol. 19, No. 3, 2003, pp. 424-430. doi: 10.2514/2.6125
[22]Ruchti, C. B., and Niemeyer, L., "Ablation Controlled Arcs," *IEEE Transactions on Plasma Science*, Vol. PS-14, No. 4, 1986, pp. 423-434. doi: 10.1109/TPS.1986.4316570
[23]Schönherr, T., Komurasaki, K., and Herdrich, G., "Propellant Utilization Efficiency in a Pulsed Plasma Thruster," *Journal of Propulsion and Power*, Vol. 29, No. 6, 2013, pp. 1478-1487. doi: 10.2514/1.B34789
[24]Seeger, M., Tepper, J., Christen, T., and Abrahamson, J., "Experimental Study on Ptfe Ablation in High Voltage Circuit-Breakers," *Journal of Physics D: Applied Physics*, Vol. 39, No. 23, 2006, pp. 5016-5024. doi: 10.1088/0022-3727/39/23/018
[25]Wang, W., Kong, L., Geng, J., Wei, F., and Xia, G., "Wall Ablation of Heated Compound-Materials into Non-Equilibrium Discharge Plasmas," *Journal of Physics D: Applied Physics*, Vol. 50, No. 7, 2017. doi: 10.1088/1361-6463/aa5606
[26]Glascock, M. S., Rovey, J. L., and Polzin, K. A., "Electric Solid Propellant Ablation in an Arc Discharge," *Journal of Propulsion and Power*, 2019, pp. 1-10. doi: 10.2514/1.B37517
[27]Glascock, M. S., Rovey, J. L., Williams, S., and Thrasher, J., "Plume Characterization of Electric Solid Propellant Pulsed Microthrusters," *Journal of Propulsion and Power*, Vol. 33, No. 4, 2017, pp. 870-880. doi: 10.2514/1.B36271
[28]Glascock, M. S., "Characterization of Electric Solid Propellant Pulsed Microthrusters." Vol. M.S., Missouri University of Science and Technology, 2016.
[29]Wilson, M. J., Bushman, S., and Burton, R. L., "A Compact Thrust Stand for Pulsed Plasma Thrusters," *25th International Electric Propulsion Conference*, ERPS, Cleveland, OH, 1997.
[30]Polk, J. E., Pancotti, A., Haag, T., King, S., Walker, M. L. R., Blakely, J., and Ziemer, J., "Recommended Practice for Thrust Measurement in Electric Propulsion Testing," *Journal of Propulsion and Power*, Vol. 33, No. 3, 2017, pp. 539-555. doi: 10.2514/1.B35564

[31]Glascock, M. S., Rovey, J. L., and Polzin, K. A., "Impulse Measurements of Electric Solid Propellant in an Electrothermal Ablation-Fed Pulsed Plasma Thruster," *2019 Joint Propulsion Conference*, AIAA, Indianapolis, IN, 2019.